Angewandte Chemie
Eine Zeitschrift der Gesellschaft Deutscher Chemiker

Supporting Information

69451 Weinheim, Germany

Raman spectroscopic study of the phase transition of amorphous to •-carbonic acid**

Ingrid Kohl, Katrin Winkel, Marion Bauer, Klaus R. Liedl, Thomas Loerting,* and Erwin Mayer

Methods:

For the spectra shown in Figure 1, H_2CO_3 films were prepared on a ZnSe window (13x2 mm) by depositing sequentially at 78 K layers of glassy aqueous solutions of 0.1 M $KHCO_3$ and 1 M HBr in the form of droplets. For the spectra of Figure 2, 2 M $KHCO_3$ and 4 M HBr solutions were deposited on an Amtir window. For details of the technique see ref. [21], and for a schematic drawing of the apparatus ref. [46]. The latter was equipped in addition with two KBr windows for following by FTIR spectroscopy spectral changes of the film deposited on the cryoplate on heating. We found that recording of Raman spectra of H_2CO_3 films requires thicker films than those necessary for recording IR spectra. Because of that, altogether 7 layers were deposited sequentially, starting and finishing with a layer of acid. The films were then heated in vacuo (~10^{-7} mbar) from 78 K to a selected temperature to induce protonation of HCO_3^-, and removal of water and excess HBr. Removal of solvent, protonation of HCO_3^-, and phase transition of amorphous to β-H_2CO_3 was first followed by FTIR spectroscopy on heating of the films in steps. IR spectra for Figure 1 were recorded in transmission on Biorad´s FTS 45 at 2 cm^{-1} resolution, by coadding 256 scans.[21] IR spectra for Figure 2 were recorded on a Varian Excalibur FTIR spectrometer. After characterizing a film by its IR spectrum, cryoplate and film were transferred under liquid nitrogen to a cryostat used for recording Raman spectra at ~80 K and ~10 mbar.

Raman spectra were recorded at 80 K on a Labram-1B spectrometer equipped with a microscope (from Dilor), through a ULWD-50 objective (Olympus). A 20 mW He-Ne laser operating at 632.8 nm was used. The 1800 g(grooves) mm^{-1} grating provides a resolution of ~2 cm^{-1}. Higher signal-to -noise ratio was obtainable with the 600 g mm^{-1} grating, and therefore this was used for survey spectra and for following the phase transition. However, since the theoretical resolving power is proportional to the number of grooves of the grating,[47] resolution with the 600 g mm^{-1} grating is much less than that of the 1800 g mm^{-1} grating. For the 1800 g mm^{-1} (600 g mm^{-1}) grating, four (three) sets of spectra were coadded with an overall recording time of 13 (5) min. The abscissa was calibrated with a silicon standard, and the sharp Raman shifts are accurate to ±2 cm^{-1} for the 1800 g mm^{-1} grating. Relative intensities of bands in different parts of the figures are not shown on the same scale. An Oxford Microstat was used as cryostat. The temperature of the sample was controlled by a LakeShore CI330 autotuning temperature controller and remained constant to within ±0.2 K.

In order to test our suggestion of a local center of symmetry we have calculated harmonic vibrational frequencies for the syn-syn, syn-anti and anti-anti carbonic acid monomers and the cyclic carbonic acid dimer. Whereas none of the monomers shows a center of inversion, such a center is present in the cyclic dimer. Since Raman and IR spectroscopy both probe mainly local interactions, we expect a reasonable agreement for the uncoupled internal modes in the cyclic dimer with the IR/Raman modes even though we are comparing a gas-phase calculation with solid-state spectra. Indeed both the number of peaks and the harmonic frequencies are in reasonable agreement with the experiment. Also the normal-modes, which we assigned on the basis of comparing our solid-state spectra with other dicarboxylic acids (see next section), agree very well with the calculated normal-modes in the cyclic dimer. By contrast, we expect no agreement between the gas-phase monomer calculations and the solid-state spectra. Also this expectation is confirmed. A gas-phase monomer calculation can not explain the number of peaks observed in solid-state spectra, and the harmonic frequencies as well as the normal-modes do not match at all. Both geometry optimization and calculation of the Hessian matrix were done at the MP2/aug-cc-pVDZ level of theory. The external hydrogen atoms were assigned an arbitrarily high-mass of 1000 amu, which corresponds to tethering the gas-phase dimer to a “wall”. Since the normal-modes strongly coupled to the external hydrogen atoms are shifted to <200 cm^{-1} this procedure helps in identifying normal-modes which are strongly coupled to intermolecular modes (not entering gas-phase calculations). These strongly coupled modes are of no interest in Table 1 because agreement between these modes and solid-state spectra is not

expected. In addition to these strongly coupled modes there are a few less strongly coupled modes (namely the Ag-band at 973 cm^{-1} and the Bu-band at 974 cm^{-1} shown in the Supporting Figure, which oscillate at 1234 cm^{-1} and 1238 cm^{-1} in the free dimer and an out-of-plane mode, which shifts from 580 cm^{-1} to 426 cm^{-1}). All other gas-phase normal modes (listed in Table 1) are barely coupled to the external hydrogen atoms (i.e., the peak-position does not significantly depend on the mass assigned to the external hydrogen atoms in the cyclic dimer). That is, for these modes the local gas-phase dimer vibrational structure provides a very reasonable estimate for the solid-state Raman and IR spectra. These normal-modes can be employed to assist band assignment in cases where a comparison to other (di)carboxylic acids does not help.

Band Assignment:

Assignment of the Raman bands to normal modes of a particular symmetry type is not meaningful because not only intermolecular hydrogen bonding, but also the monomer conformation is an important factor for crystal packing. Therefore, the assignment can only be attempted by a qualitative description of the modes, similar to that of IR spectra of β-H_2CO_3,[10-15, 19, 20, 22, 24] and it is based on comparisons with assignments of other crystalline carboxylic acids and on our calculation of the harmonic frequencies in the cyclic carbonic acid dimer. We note that strong coupling between the various modes is often observed for carboxylic acid dimers which makes vibrational assignments in terms of distinct modes even less meaningful.[36, 48, 49] Peak positions of IR and Raman bands and several tentative vibrational assignments are listed in Table 1 (where ν_s and ν_{as} are symmetric and antisymmetric stretching modes, δ_{ip} and δ_{oop} are in-plane and out-of-plane bending modes.vs, s, m, w, vw and sh stand for very strong, strong, medium, weak, very weak and shoulder) on the basis of a local center of symmetry and discussed as follows.

The weak Raman band centered in amorphous H_2CO_3 at ~1642 cm^{-1} shifts on phase transition to β-H_2CO_3 to ~1605 cm^{-1} (Figure 1(b) and 1(f)). We assign this band to the C=O stretching vibration. The C=O stretching mode of the carboxylic acid dimer is generally observed to be strong in the IR and weak in the Raman,[49] which is consistent with relative intensities of the IR and Raman band of β-H_2CO_3 (see Figure 2). For β-H_2CO_3 containing a local center of symmetry, the Raman band must be symmetric (ν_sC=O), whereas the IR band must be antisymmetric (ν_{as}C=O). The large splitting,Δν(C=O), between the Raman ν_sC=O mode and the IR ν_{as}C=O mode is characteristic for carboxylic acid dimers[36] and has been examined theoretically for the formic acid dimer.[50] The Δν(C=O) value of more than 90 cm^{-1} is consistent with Δν(C=O) = 100 cm^{-1} obtained in density functional calculations of the carbonic acid dimer,[40] and of 57 (65) cm^{-1} in our calculation of harmonic frequencies (Table 1).

The band centered in amorphous H_2CO_3 at ~1506 cm^{-1} shifts on crystallization to ~1540 cm^{-1} (Figure 1(b) and 1(f)). The band at 1376 cm^{-1} shifts on crystallization to 1400 cm^{-1}. A characteristic band in the Raman spectra of dimeric carboxylic acids is the in-plane OH deformation (δ_{ip}(COH) at 1430-1410 cm^{-1} (ref. [51])). This mode is coupled with the C-O stretching mode (ν(C-O)) according to extensive Raman spectroscopic studies and calculations of malonic acid and its isotopomers.[48, 52] The intense band centered in amorphous H_2CO_3 at 1045 cm^{-1} shifts on crystallization only slightly to higher wavenumbers (Figure 1(b) and 1(f), and Figure 2(c)). Our normal-mode calculation allows to assign this band to a simultaneous stretching vibration of two C-O bonds and the C=O bond. Raman spectra of other dicarboxylic acids do not show an intense band in this spectral region since they do not contain a CO_3-group. The three-band system in amorphous H_2CO_3 centered at 673, 620 and 587 cm^{-1} develops on phase transition to β-H_2CO_3 into a two-band system (Figure 1(b) and 1(f)). In a mixture of amorphous and β-H_2CO_3 the five bands are clearly separated (Figure 1(d)). The weak band at 676 cm^{-1} in Figure 1(f) indicates a minor amount of amorphous H_2CO_3 in β-H_2CO_3. The two bands at 650 and 598 cm^{-1} (657 and 605 cm^{-1} in Figure 2(c)) are assigned according to refs. [36, 48, 52], and to our calculations to COO bending (δ(COO)) and skeletal bending modes.

The two intense bands centered at 193 and 256 cm^{-1} are already in the spectral region where lattice modes are possible. The lower limit for internal modes in a dicarboxylic acid is around 250 cm^{-1},[48] and thus the band at 256 cm^{-1} could be an internal

mode, whereas the band at 193 cm^{-1} could be an external mode which can be coupled with internal modes. Table 3 in ref. [48] gives examples for coupling of external and internal modes in crystalline malonic acid. Raman spectra of isotopomers of β-H_2CO_3 are necessary before we can attempt assignment of these two bands.

The Raman band centered in Figure 2(c) at ~3097 cm^{-1} (at ~3089 cm^{-1} in Figure 2 (b)) we attribute to the O-H stretching vibration of hexagonal ice (ice Ih)[53] which had condensed onto the film during transfer of film and disk from the IR apparatus to the Raman microstat. In the band-narrowed second derivative a weak band centered at 223 cm^{-1} becomes observable which can be assigned to the translational mode of ice Ih.[54] The band at ~3089 cm^{-1} is also observable in the Raman spectrum of β-D_2CO_3 (not shown) which is consistent with our assignment of this band to ice Ih. Thus, the O-H stretching band in the Raman spectrum of β-H_2CO_3 could be either hidden by the band from ice Ih, or it could be too weak to be detectable with our spectrometer. We note that the carboxylic acid OH stretching bands are generally weak in the Raman spectrum.[49]

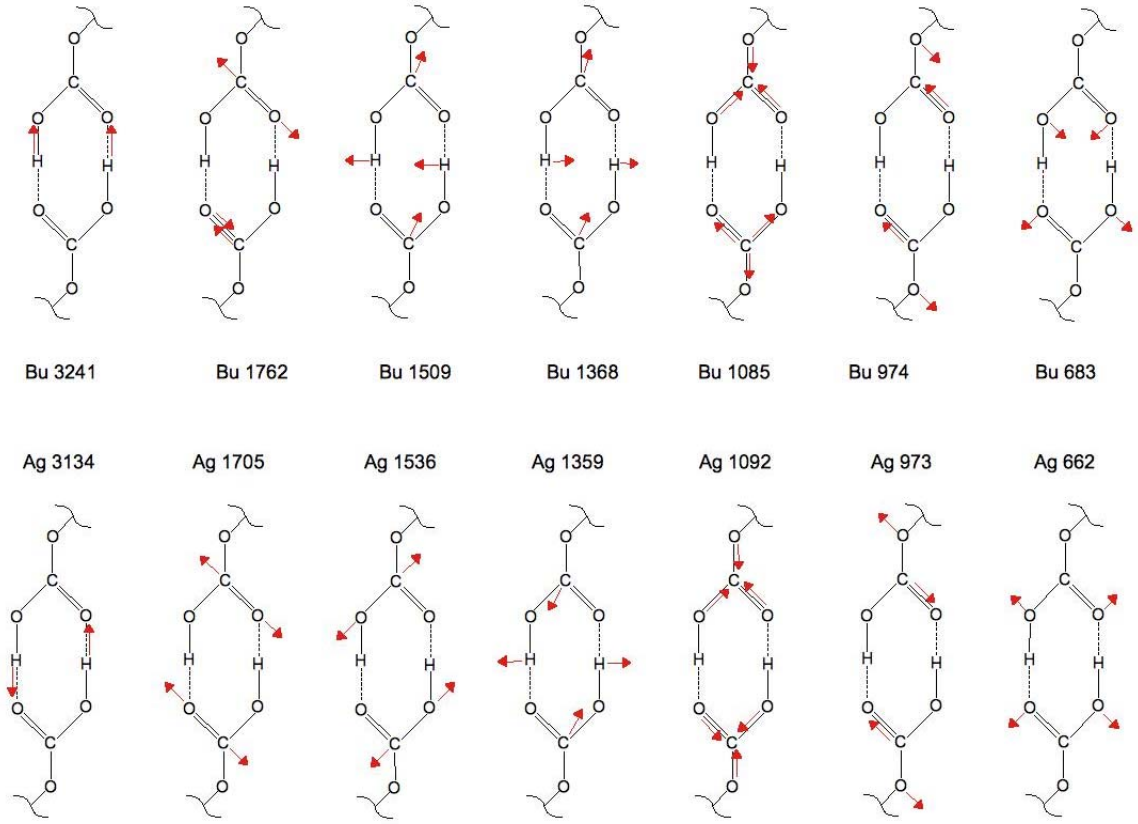

Supporting Figure: Schematic representation of in-plane normal modes in the tethered carbonic acid dimer of C_{2h}-symmetry as calculated at MP2/aug-cc-pVDZ level of theory and by assigning a mass of 1000 amu to the external hydrogen atoms (represented as a wall). Compensating motions, which avoid a shifting center of gravity, are omitted for clarity.

Band Calibration:

In the Raman spectrum recorded at high resolution (Figure 2c), the plasma-line of the He-Ne laser centered at 180.4 cm^{-1} (ref. [34]) is resolved from the intense band at 193 cm^{-1}. Thus we can exclude that the intense band centered at 193 cm^{-1} is a plasma-line. The plasma-line at 180.4 cm^{-1} serves as an *in situ* calibration band and therefore, peak positions in Figure 2c are the most reliable ones, whereas the increased S/N ratio at low resolution (Figure 2b) helps in searching for Raman bands of low intensity.

Experimental Details

In such a comparison of IR and Raman spectra shown in Figure 1, a problem can arise because IR spectra are recorded from a disc with ~10 mm diameter, whereas the spatial resolution of Raman spectra recorded through a microscope is in the μm range. Thus, the Raman spectrum recorded from a μm-sized spot might not be characteristic of the spectrum averaged over a 10-mm diameter disc. This is observable in a comparison of the spectra recorded after heating to 190 K where the IR spectrum indicates already formation of a small amount of β-H_2CO_3 (Figure 1a) whereas in the corresponding Raman spectrum the bands of β-H_2CO_3 (Figure 1b) are absent. To avoid that problem, we have recorded Raman spectra from many different spots of the film, and found that peak positions of the Raman spectra shown in Figure 1b, 1d and 1f are characteristic for each temperature over the whole film, only relative intensities of the bands assigned to amorphous/β-H_2CO_3 vary somewhat.
A weak band centered in Figure 1a and 1c at 1033 cm^{-1} disappears on further heating to 210 K (Figure 1e). This band was not observed in our previous IR spectral study.[24] It could be from a minor amount of β-H_2CO_3, whose peak position is shifted by interaction with the matrix in the thick film.

In our recent IR-spectroscopic study of the phase transition of the two amorphous forms of H_2CO_3 to α- and β-H_2CO_3 we had emphasized "that the main spectral features in the IR spectra of α- and β-H_2CO_3 are observable already in those of the amorphous H_2CO_3 forms. This indicates that H-bond connectivity or conformational state in the two crystalline phases is on the whole already developed in the two amorphous forms".[24] The same holds for this Raman spectroscopic study because peak positions and relative intensities of amorphous H_2CO_3, called β-amorph in ref. [24], are remarkably similar to those of β-H_2CO_3 (see Figure1b and 1f).

References

[10] M. H. Moore, R. K. Khanna, *Spectrochimica Acta, Part A: Molecular and Biomolecular Spectroscopy* **1991**, *47A*, 255.
[11] M. H. Moore, R. Khanna, B. Donn, *Journal of Geophysical Research, [Planets]* **1991**, *96*, 17541.
[12] N. DelloRusso, R. K. Khanna, M. H. Moore, *J. Geophys. Res.* **1993**, *98*, 5505.
[13] J. R. Brucato, M. E. Palumbo, G. Strazzulla, *Icarus* **1997**, *125*, 135.
[14] P. A. Gerakines, M. H. Moore, R. L. Hudson, *Astronomy and Astrophysics* **2000**, *357*, 793.
[15] G. Strazzulla, G. A. Baratta, M. E. Palumbo, M. A. Satorre, *Nuclear Instruments & Methods in Physics Research, Section B: Beam Interactions with Materials and Atoms* **2000**, *166-167*, 13.
[19] W. Hage, A. Hallbrucker, E. Mayer, *Journal of the Chemical Society, Faraday Transactions* **1995**, *91*, 2823.
[20] W. Hage, A. Hallbrucker, E. Mayer, *Journal of the Chemical Society, Faraday Transactions* **1996**, *92*, 3197.
[21] W. Hage, A. Hallbrucker, E. Mayer, *Journal of the Chemical Society, Faraday Transactions* **1996**, *92*, 3183.
[22] W. Hage, A. Hallbrucker, E. Mayer, *Journal of Molecular Structure* **1997**, *408-409*, 527.
[24] K. Winkel, W. Hage, T. Loerting, S. L. Price, E. Mayer, *J. Am. Chem. Soc.* **2007**, *129*, 13863.
[34] J. R. Ferraro, K. Nakamoto, *Introductory Raman Spectroscopy*, Academic Press, London, **1994**.
[36] I. Wolfs, H. O. Desseyn, *Appl. Spectroscopy* **1996**, *8*, 1000.
[40] P. Ballone, B. Montanari, R. O. Jones, *Journal of Chemical Physics* **2000**, *112*, 6571.
[46] I. Kohl, L. Bachmann, A. Hallbrucker, E. Mayer, T. Loerting, *Phys. Chem. Chem. Phys.* **2005**, *7*, 3210.
[47] B. Schrader, in *Infrared and Raman Spectroscopy. Methods and Applications* (Ed.: B. Schrader), VCH, Weinheim, **1995**, pp. 63.
[48] D. Bougeard, J. deVillepin, A. Novak, *Spectrochim. Acta* **1988**, *44A*, 1281.
[49] D. Lin-Vien, N. B. Colthup, W. G. Fateley, J. G. Grasselli, *The Handbook of Infrared and Raman Characteristic Frequencies of Organic Molecules*, Academic Press, New York, **1991**.
[50] W. Qian, S. Krimm, *J. Phys. Chem.* **1996**, *100*, 14602.
[51] F. R. Dollish, W. G. Fateley, F. F. Bentley, *CHARACTERISTIC RAMAN FREQUENCIES OF ORGANIC COMPOUNDS*, Wiley, New York, **1974**.
[52] J. deVillepin, M.-H. Milage, A. Novak, N. Toupry, M. LePostollec, H. Poulet, S. Ganguly, C. N. R. Rao, *J. Raman Spectroscopy* **1984**, *15*, 41.
[53] P. T. T. Wong, E. Whalley, *J. Chem. Phys.* **1975**, *62*, 2418.
[54] P. T. T. Wong, E. Whalley, *J. Chem. Phys.* **1976**, *65*, 829.